行政院國家科學委員會專題研究計畫　成果報告

子計畫一：靜電式微機電振動-電能轉換器

計畫類別：整合型計畫
計畫編號：NSC94-2215-E-009-057-
執行期間：94年08月01日至95年07月31日
執行單位：國立交通大學電機與控制工程學系(所)

計畫主持人：邱一

計畫參與人員：郭炯廷　曾繁果

報告類型：精簡報告
報告附件：出席國際會議研究心得報告及發表論文
處理方式：本計畫可公開查詢

中　華　民　國 95年10月31日

一、研究計畫中英文摘要：

摘要

可攜式或遠距使用(remote)的電子產品或系統的電源除了由電池來供應外，目前國外許多學者正嘗試以功率微機電（power MEMS）的技術，將各種化學能或動能轉換成電能，以做為微型的整合型電源供應(micro integrated power supply)。

本計畫採用靜電式的動能-電能轉換方式，已於前一年度完成系統模擬及設計出輸出功率 20μW 的電源供應器，並完成了第一代元件的製作及測試。本年度計畫除改善第一代元件的設計及製程缺失外，著重於大幅增加元件的可變電容值，並針對測量到的 120 Hz, 2.25 m/s^2 的振動，在 3.3 V 輔助電源的條件下，於 1 cm^2 的晶片面積上設計出一淨輸出超過 200 μW 的微型電源供應器。

目前已完成元件的靜態及動態模擬，以及在 SOI 基板上的製作。電性及機械特性測試則正在進行中。

關鍵詞：功率微機電系統；能量轉換；振動；靜電式；駐極體；智慧型微感測系統

Abstract

Portable or remote electronic devices are powered by batteries traditionally. Recently, there are increasing interests in the development of micro integrated power supply, which converts various energy sources, such as chemical and kinetic, to electricity using the power MEMS technology.

The objective of this project is to develop an electrostatic MEMS vibration-to-electric energy converter within an area of 1 cm^2 based on a 3.3 V auxiliary power supply. The targeted energy source is the 120 Hz, 2.25 m/s^2 vibration measured in household appliances. In the previous year, such a device with 20 μW net power output was designed and fabricated. The targets of this year are to solve the fabrication issues found in the first-generation device, and to develop a 200 μW-output device by improved capacitor design.

The static and dynamic analyses have been accomplished. The device was fabricated in a SOI wafer and is currently under electrical and mechanical testing.

Keywords：power MEMS, energy conversion, vibration, electrostatic, electrete, smart micro sensor system

二、研究計畫內容：

(一) 研究計畫之背景及目的

Due to the advance of CMOS VLSI technology, the power consumption of electronic devices has been reduced considerably. The low power technology enables the development of such applications as wireless sensor networks [1] or personal health monitoring [2], where remote or independent power supply is critical for more compact or longer-life-time systems. In particular, energy scavenging from ambient natural sources, such as vibration [3], radioisotope [4] and ambient heat [5], is attracting many recent interests as the self-sustainable power source for these applications. Among various approaches, electrostatic vibration-to-electricity conversion using the micro-electro-mechanical systems (MEMS) technology is chosen in this study due to its compatibility to IC processes and the ubiquity of the energy source in nature.

The output power of a vibration driven converter is related to the nature of the vibration source. A typical vibration found in many household appliances has a peak acceleration of about 2.25 m/s^2 at about 120 Hz. Therefore, this vibration is used as the energy source for the design of the optimal converter.

（二）研究計畫之方法及結果

1．Design

A variable capacitor C_v formed by an in-plane gap-closing comb structure is the main component in the energy converter [3, 6], as shown in Fig. 1. The energy stored in the capacitor is increased when the capacitance is changed from C_{max} to C_{min} by the external vibration. Fig. 2 shows a schematic circuit that can be used to extract the converted energy.

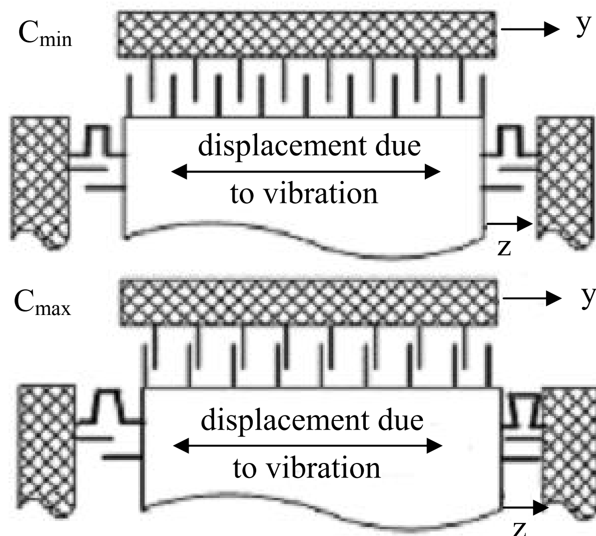

Figure 1 Variable capacitor schematic

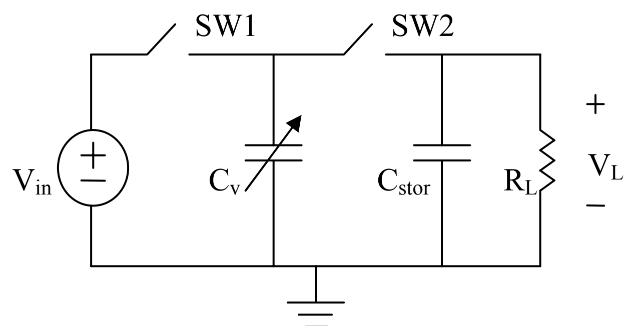

Figure 2 Operation of the electrostatic energy converter

The variable capacitor C_v is charged by an external voltage source V_{in} through the switch SW1 when C_v is at its maximum $C_{max.}$ When C_v is charged to V_{in}, SW1 is opened and then the

capacitance is changed from C_{max} to C_{min} due to the electrode displacement caused by vibration. In this process, the charge Q on the capacitor remains constant (SW1 and SW2 both open). Therefore, the terminal voltage on the capacitor is increased and the vibration energy is converted to the electriostatic energy stored in the capacitor. When the capacitance reaches C_{min} (V_{max}), SW2 is closed and the charge is transferred to a storage capacitor C_{stor}. SW2 is then opened and C_v varies back to C_{max}, completing one conversion cycle. During this period, the charge on C_{stor} is discharged by the load resistance R_L with time constant $\tau = C_{stor}R_L$ before it is charged again by C_v. In the steady state, the initial and final terminal voltages V_L of the discharge process become constnat, as shown in Fig. 3.

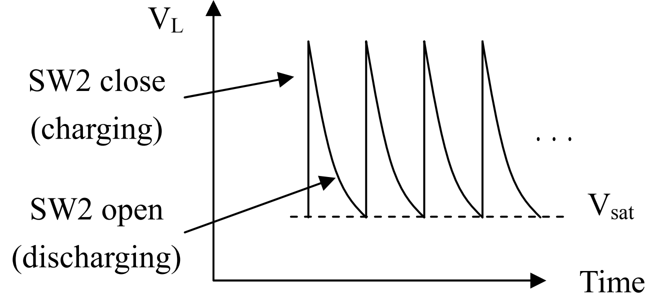

Figure 3 Output terminal voltage V_L

It can be shown that the steady-state final terminal voltage V_{sat} in the chrage-discharge cycle can be expressed as

$$V_{sat} = \frac{\frac{C_{max}}{C_{stor}} V_{in}}{(1+\frac{C_{min}}{C_{stor}}) \times \exp(\Delta t / R_L C_{stor}) - 1}, \qquad (1)$$

where Δt = conversion cycle time = 1/2f and f is the vibration frequency. When the voltage ripple of the charge-discharge process is small, as will be shown subsequently, the output power can be estimated by,

$$P_{out} = \frac{V_{sat}^2}{R_L}, \qquad (2)$$

which is in general proportional to C_{max}^2. In the comb structure of the variable capacitor, C_{max} is determined by the minimum finger spacing, which was kept at 0.5 μm to prevent shortage of the uninsulated fingers in the previous design [7]. If a dielectric coating can be applied to the side walls to insulate the fingers (Fig. 4), the minimum spacing can be reduced to increase C_{max} and P_{out}. Silicon nitride will be used as the dielectric material due to its process compatibility and high dielectric constant (ε_r=7). It should be noted that the dielectric coating barely increases C_{min}. Therefore, the expected increase of output power will not be affected by the change of C_{min}.

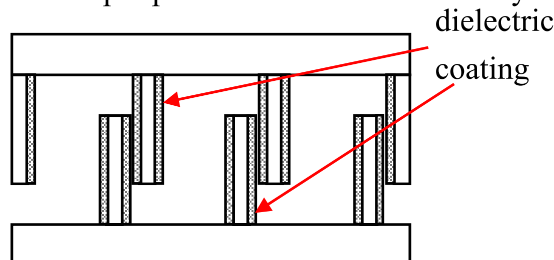

Figure 4 Variable capacitor at C_{max} position with dielectric coating

1.1 Static analysis

In Eq. (1), R_L and C_{stor} can be choosen so that the discharging time constant $\tau = C_{stor}R_L$ is much larger than the conversion cycle time Δt. The output voltage ripple in the steady state can therefore be neglected. The other circuit components can then be choosen so that $C_{stor} >> C_{min}$ and $R_L C_{min} << \Delta t$ and Eq. (1) can be simplified as

$$V_{sat} \approx \frac{\frac{C_{max}V_{in}}{\Delta t}}{C_{min}\frac{\Delta t}{R_L C_{min}}} = \frac{C_{max}V_{in}}{\Delta t} R_L, \qquad (3)$$

The power output becomes

$$P_{out} \approx \frac{V_{sat}^{2}}{R_L} \approx \left(\frac{C_{max}V_{in}}{\Delta t}\right)^2 R_L, \qquad (4)$$

For a typical low-power sensor node or module, the minimum output power requirement is about 200 μW. To be compatibile with the power management circuit, the maximum output voltage should be limited to about 40 V. Inserting these constraints into Eq. (2), one can obtain the range of R_L:

$$R_L \le 8\ \mathrm{M\Omega}\,.$$

Even though a smaller R_L can be used, this would require increasing C_{max} in order to satisfy the voltage and power requirement (Eqs. (3) and (4)), which in turn will have adverse effects in the dynamic behavior of the converter. Therefore, $R_L = 8\ \mathrm{M\Omega}$ and hence $C_{max} = 7$ nF are used in the following calculation.

The output power P_{out} for various C_{stor} and R_L is shown in Fig. 5 for $C_{stor} >> C_{min}$. It can be seen that the output power does not depend on the storage capacitor C_{stor} when it is relatively large. Nevertheless, a large C_{stor} will result in long initial charge time when the converter starts to work from a static status. Hence, a resonable C_{stor} of 20 nF is used.

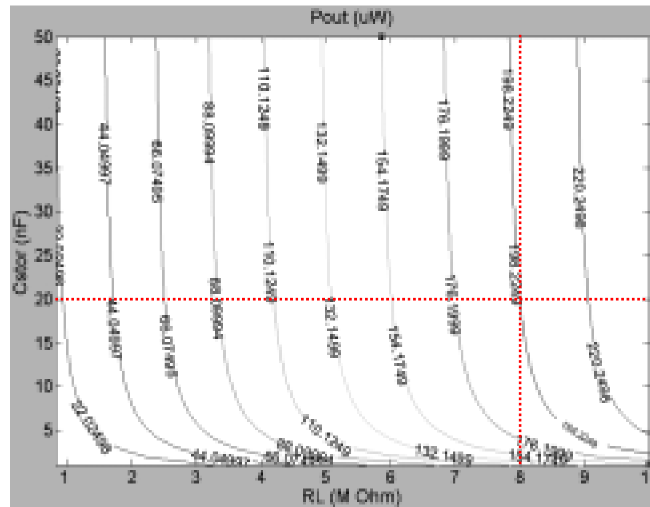

Figure 5 Output power for various R_L and C_{stor}

From Eq. (1) and with the values of C_{stor} and R_L obtained from above, input voltage V_{in} of 3.3 V, vibration frequency of 120 Hz, and chip area size of 1 cm^2, Fig. 6 shows the calculated output saturation voltage and power as a function of the initial finger gap distance and the thickness of the silicon nitride layer. The finger thickness, length, and width are 200 μm, 1200 μm

and 10 μm, repsectively [7]. The dimension of the fingers are based on the available deep etching process capability. The minimum gap distance is assumed to be 0.1 μm, which is controled by mechanical stops. It can be seen that with a 500-Å-thick nitride, the initial finger gap has an optimal value of 35 μm for a power output of 200 μW and output voltage of 40 V.

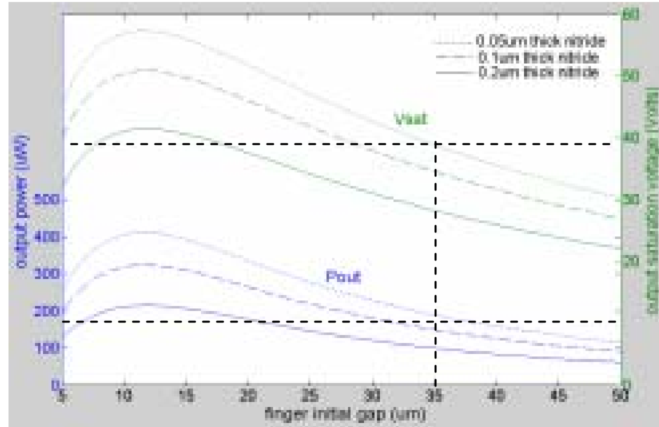

Figure 6 Output saturation voltage and power vs. initial finger gap ($R_L = 8\ M\Omega$, $C_{stor} = 20$ nF)

1.2 Dynamic analysis

After the dimension of the variable capacitor is determined from the static analysis, the dynamics of the micro structure is analyzed so that the desired maximum displacement, and hence C_{max}, can be achieved by the target vibration source. The electro-mechanical dynamics of the converter can be modeled as a spring-damper-mass system. The dynamic equation is

$$m\ddot{z}+b_e(z)+b_m(z,\dot{z})+kz=-m\ddot{y}, \qquad (5)$$

where z is the displacement of the shuttle mass m with respect to the device frame, y is the displacement of the device frame caused by vibration, $b_m(z,\dot{z})$ is the equivalent mechanical damping representing energy loss caused mainly by the squeezed film effect, and $b_e(z)$ is the equivalent electrical damping representing the electrostaitc force acting on the MEMS structure. Notice that the mechanical damping force, $b_m(z,\dot{z})$, is a function of both the displacement z of the shuttle mass and its velocity $\dot{z}$ [3].

A Simulink model was built to simulate the system behavior based on Fig. 2 and Eq. (5) as shown in Figure 7. Due to the limited shuttle mass that can be achieved in a MEMS process using only silicon, an external attached mass m is considered in order to increase the displacement of the variable capacitor and the energy conversion efficiency.

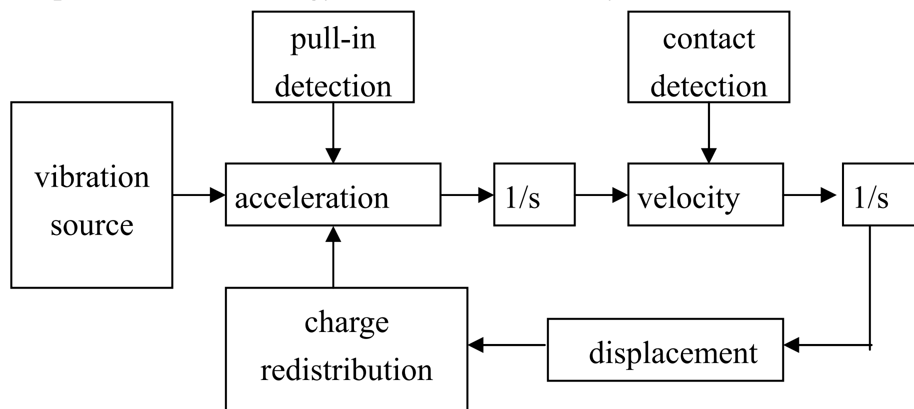

Figure 7 Dynamic simulation frame

From the Simulink simulation, a mass of 7.2 gram is required to achieve the maximum displacement of 34.8 μm according to the static design with a corresponding spring constant of 4.3 kN/m. The output voltage as a function of time is plotted in Fig. 8. The charging-discharging cycles and voltage ripples are evident and the saturation voltage V_{sat} is close to the expected value of 40 V. Table 1 summarizes the important device design parameters according to both the static and dynamic analyses.

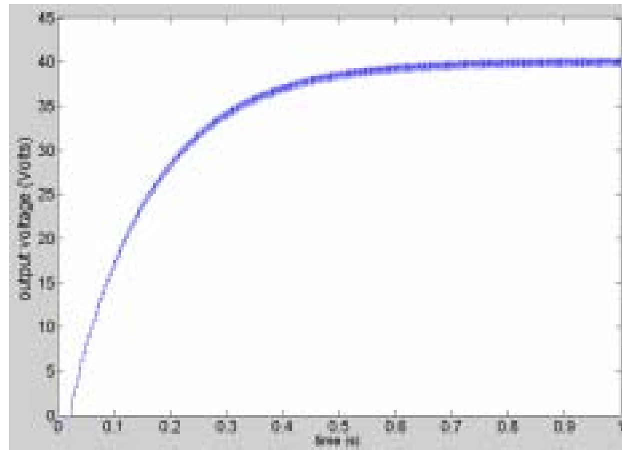

Figure 8 Output voltage vs. time

Table 1 Design parameters of the energy converter

Parameter	Description	
W	Width of shuttle mass	10 mm
L	Length of shuttle mass	8 mm
L_f	Length of finger	1200 μm
W_f	Width of finger	10 μm
m	Shuttle mass	7.2 gram
d	Initial finger gap	35 μm
d_{min}	Minimum finger gap	0.1 μm
C_{stor}	Storage capacitance	20 nF
k	Spring constant	4.3 kN/m
t	Dielectric layer thickness	500 Å
ε_r	Dielectric constant	7 (SiN)
R_L	Load resistance	8 MΩ
V_{sat}	**Output voltage**	**~ 40 V**
P_{out}	**Output power**	**~ 200 μW**

2. Fabrication

A SOI wafer with a 200-μm-thick device layer is used for large capacitance. The oxide layer is 2 μm thick. Fig 9 shows the fabrication process. A steel ball is attached to the central plate to adjust the resonant frequency to match the vibration source and improve the conversion efficiency . The fabricated second-generation device is shown in Fig. 10 [7]. The width of the finger is reduced to 9.5 μm due to the tolerance in photolithography and RIE processes.

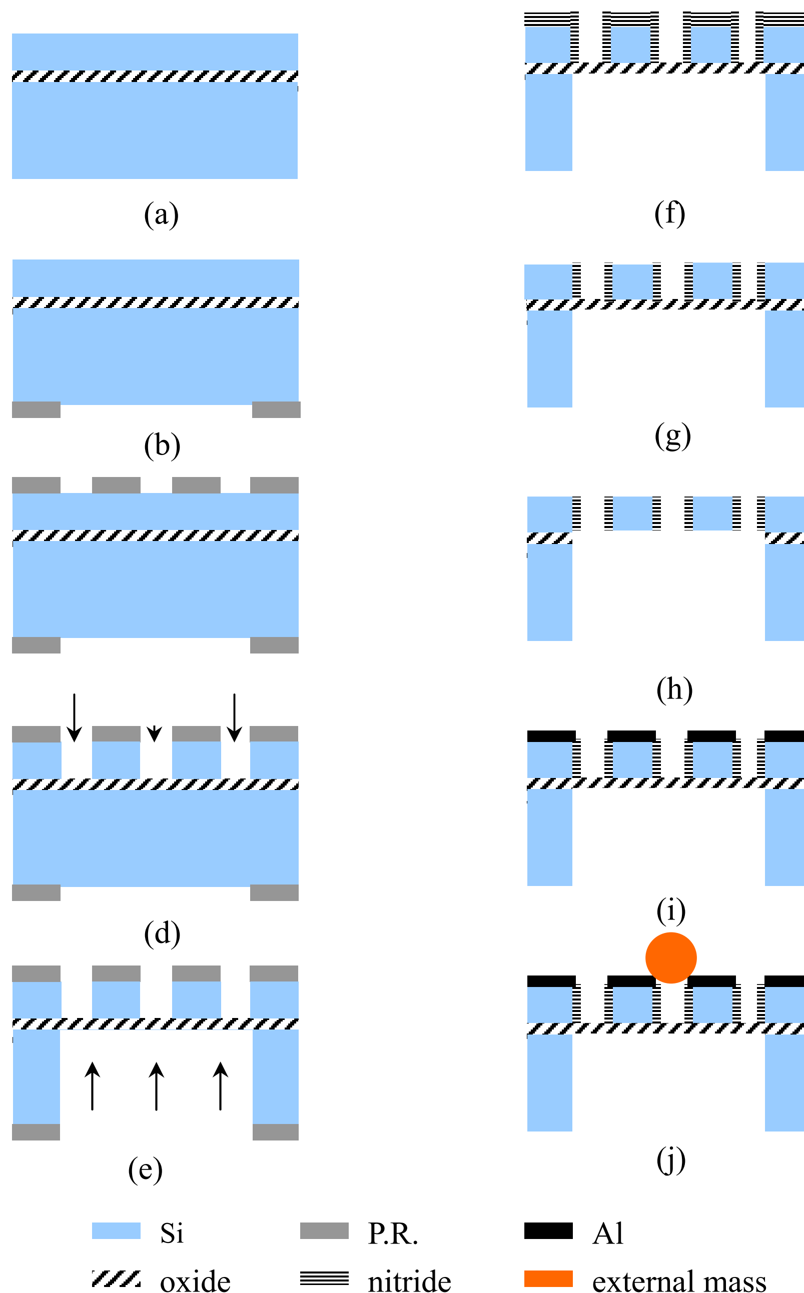

Figure 9 Processing steps: (a) start from a SOI wafer, (b) coat and pattern backside P.R., (c) coat and pattern frontside P.R., (d) etch the device layer by DRIE, (e) etch the backside by DRIE, (f) deposite silicon nitride on the finger side walls by LPCVD, (g) etch top silicon nitride layer on the frontside by RIE, (h) etch sacrificial oxide from backside by RIE, (i) apply Al by thermal coater, and (j) attach external mass

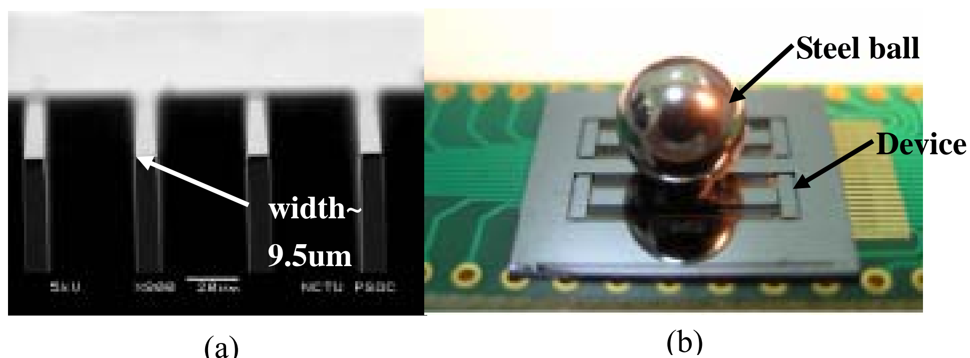

Figure10: (a) cross section of fingers (b) overview of device with external mass

3 Measurement

3.1 Mechanical measurement

The mechanical measurement setup is shown in Fig 11.The displacement of the device without the attached mass was measured using a PROWAVE JZK-1 shaker. Since the mass was not attached, the vibration acceleration was increased to 40 m/s^2 for easy observation. The maximum displacement is about 10 μm at 800 Hz, and the quality factor $Q = \omega_0/\Delta\omega$ is about 9.6, where ω_0 is the resonant frequency and $\Delta\omega$ is the resonant bandwidth shown in Fig. 12. The mass of the center plate is approximately 0.038 gram, thus the spring constant can be calculated as $k = \omega_0^2 m = 960$ N/m .The measured spring constant is different from the design mainly due to the feature size shrink in the fabrication process, as shown in Fig 9(a).

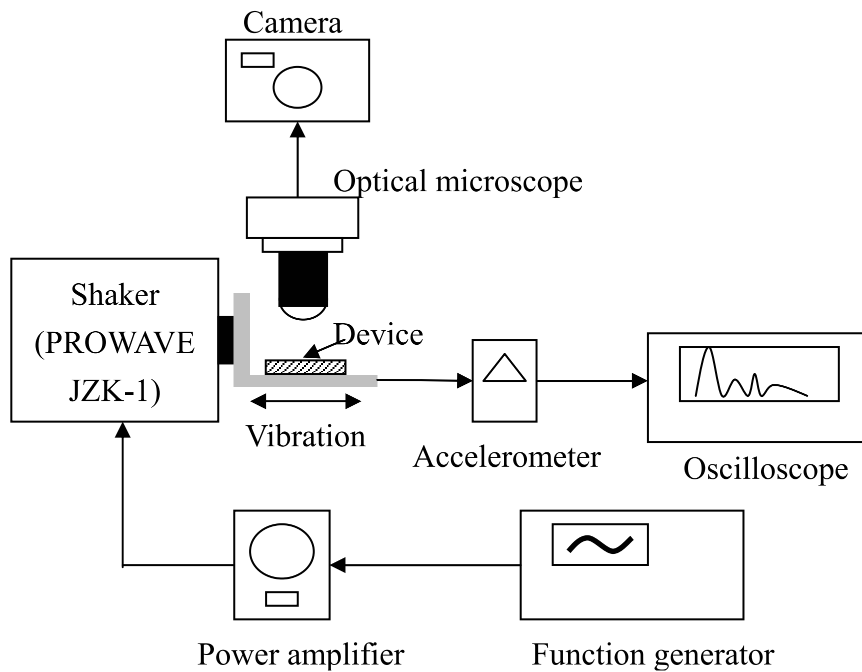

(a)

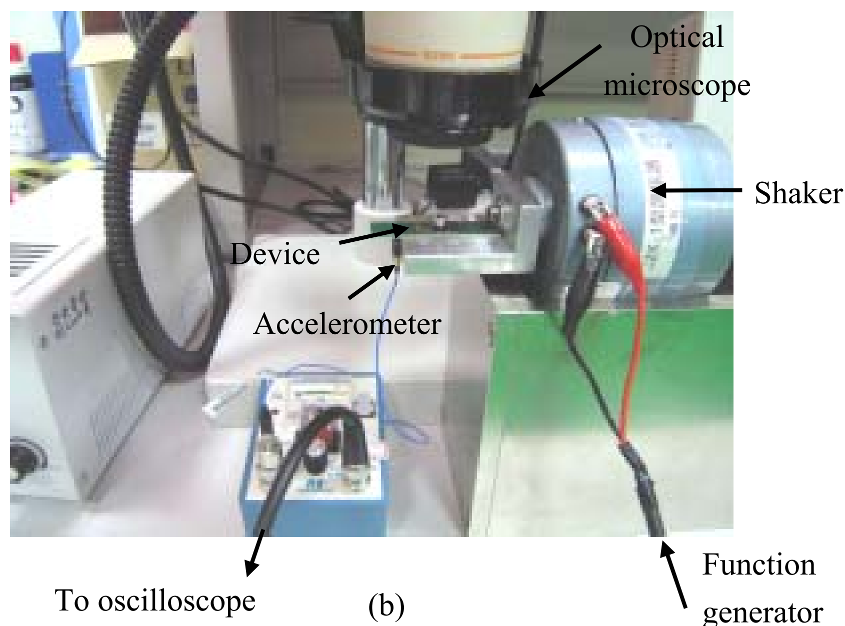

(b)

Figure 11 (a) Schematic and (b) photograph of the mechanical measurement setup

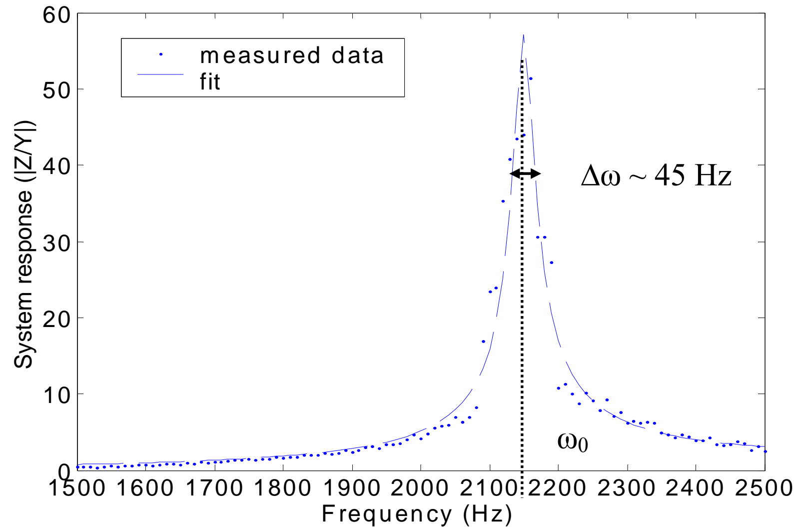

Figure 12 Measured system response

3.2 Electrical measurement

The electrical measurement was conducted using an INSTEK-LCR-816 LCR meter and a HP-4192A impedance analyzer. The measured capacitance without vibration was about 500 ~ 600 pF, while the calculated capacitance C_{min} is about 50 pf. The major contribution of the large measured capacitance is the parasitic capacitance C_{par} between the center plate and the substrate beneath it.

Besides, there is also a parallel parasitic conductance. The measured conductance varies from die to die with an average resistance of 2.5 kΩ. It is suspected to be caused by the residual particles left in the device after the release step. The presence of the parasitic capacitance and conductance had hindered the measurement of output power. New devices are being fabricated with the substrate underneath the combs and central plate removed to prevent parssitic capacitance and residual particles.

(四) 研究計畫之結果與討論

The design and analysis of a micro vibration-to-electricity converter are presented. The device was fabricated in a SOI wafer. The reduced feature size of the fabricated device resulted in the decrease of spring constants. Mechanical and electrical measurements of the fabricated device were conducted. Impedance measurements showed an unwanted parasitic conductance which resulted in the failure of output power measurement. Improvement of the design and fabrication processes is being conducted.

This project is supported in part by the National Science Council, Taiwan, ROC, under the Grant No. NSC 94-2215-E-009-057.

参考資料

[1] J.M. Rabaey, et al., “Picoradio supports ad hoc ultra low-power wireless networking”, IEEE Computer, Vol. 33, pp. 42-48, 2000.

[2] R. Tashiro, et al., “Development of an electrostatic generator that harnesses the motion of a living body: (use of a resonant phenomenon)”, JSME International Journal Series C, Vol. 43, No. 4, pp. 916-922, 2000.

[3] S. Roundy, et al., “Micro-electrostatic vibration-to-electricity converters,” Proc. IMECE 39309, 2002.

[4] R. Duggirala, et al., “Radioisotope micropower generator for CMOS self-powered sensor microsystems”, Proc. PowerMEMS 2004, pp. 133-136, 2004.

[5] T. Douseki, et al., “A batteryless wireless system uses ambient heat with a reversible-power-source compatible CMOS/SOI dc-dc converter”, Proc. IEEE International Solid-State Circuits Conference, pp. 2529-33, 2003.

[6] C.B. William, et al., “Analysis of a micro-electric generator for microsystems”, Sensors and Actuators, A52, pp. 8-11, 1996.

[7] Y.S. Chu, et al., “A MEMS electrostatic vibration-to-electricity energy converter”, Proc. PowerMEMS 2005, pp. 49-52, 2005.

附件二

可供推廣之研發成果資料表

☐ 可申請專利　　☐ 可技術移轉　　日期：95 年 10 月 30 日

國科會補助計畫	計畫名稱：靜電式微機電振動-電能轉換器 計畫主持人：邱一 計畫編號：NSC 94-2215-E-009-057　　學門領域：微電子
技術/創作名稱	考慮輸出負載影響下的靜電式振動-電能轉換器之設計方法
發明人/創作人	邱一　　郭炯廷
技術說明	中文：針對一班居家環境中振動源，進行靜電式振動-電能轉換器設計。在此使用較為常見的 120 Hz、2.25 m/s^2 振動源，並且考慮負載對輸出的充放電效應來設計更完善的系統。可變電容採用 SOI 晶圓來製作，同時用背蝕刻來移除寄生電容效應、增加轉換率。在可變電容的梳指狀結構側壁上鍍氮化矽來增加電容變化量，使最終設計之輸出功率可達 200μW。
	英文：
可利用之產業及可開發之產品	無線感測網路、個人隨身健康監控系統
技術特點	
推廣及運用的價值	在現今電子電路消耗功率越來越低的情況下，利用此種能量轉換器，將外界可利用的機械性功率轉換成電能來供整體系統使用或回充給電池，以達到近幾永續操作的性能。隨著 IC 製程技術及電子電路低功率設計越來越進步，此項技術將會越來越有利用價值。

※ 1.每項研發成果請填寫一式二份，一份隨成果報告送繳本會，一份送　貴單位研發成果推廣單位（如技術移轉中心）。

※ 2.本項研發成果若尚未申請專利，請勿揭露可申請專利之主要內容。

※ 3.本表若不敷使用，請自行影印使用。